Bending of DNA upon Binding of Ecteinascidin 743 and Phthalascidin 650 Studied by Unrestrained Molecular Dynamics Simulations

Raquel García-Nieto,[†] Ignacio Manzanares,[‡] Carmen Cuevas,[‡] and Federico Gago*[,†]

Contribution from the Departamento de Farmacología, Universidad de Alcalá, E-28871 Alcalá de Henares, Madrid, Spain, and Pharma Mar S.A., Cantoblanco, 28760 Tres Cantos, Madrid, Spain

Received March 17, 2000

Abstract: Recognition of DNA sequence information by the natural antitumor agent ecteinascidin 743 (ET743) has been proposed to operate through a direct readout mechanism involving specific hydrogen bonding interactions between the drug and the DNA minor groove prior to covalent alkylation of a guanine base. 5′-AGC and 5′-CGG are examples of high-reactivity target triplets whereas 5′-CGA is a low-reactivity sequence. Molecular dynamics computer simulations were first used to explore the stability and behavior of the pre-covalent complex between ET743 and a DNA nonamer containing the 5′-AGC binding site in the central region. The pre-covalent complex was stable, and some unreported distinctive features were observed that may not be amenable to direct experimental verification. A similar simulation with ET743 bound to another nonamer containing a central 5′-CGA triplet did not result in a stable association supporting the proposed role of a hydrogen bonding network in the stabilization of these complexes. The covalent complexes between ET743 and the nonamers containing the 5′-AGC and 5′-CGG target sites were then simulated. In each case the drug displayed the predicted binding mode and gave rise to a widening of the minor groove. In addition, we show that as a consequence of ET743 binding to the target sequences, positive roll is introduced that results in smooth bending of the helix toward the major groove, in agreement with results from gel electrophoresis experiments. Similar results were obtained with the synthetic compound phthalascidin, which presents a biological profile almost indistinguishable from that of ET743. The local bending elements in AGC and CGG were found to be different, and the distinct behavior of these sequences in the absence of bound drugs was in consonance with their intrinsic bending propensities.

Introduction

Ecteinascidin 743 (ET743) is a potent antitumor natural product[1] presently in clinical trials which consists of three linked tetrahydroisoquinoline subunits and an active carbinolamine functional group (Figure 1). Upon binding to DNA, ET743 undergoes a nucleophilic attack by the exocyclic amino group at position 2 of guanine.[2] Guanine adduct formation is influenced by the nature of the bases flanking the alkylation site and is reversible upon DNA strand separation.[3] Recognition of DNA sequence information by ET743 has been proposed to operate through a direct readout mechanism involving specific hydrogen bonding donor−acceptor pairs between the A and B subunits of the drug and a DNA triplet made up of the base pair containing the guanine that is alkylated (G) plus one flanking base pair on either side.[4,5] For a target sequence 5′-XGY, the specificity rules proposed by Seaman and Hurley establish that Y is preferentially a G or a C. If it is a G, the preferred base for X is a pyrimidine, be it T or C. If Y is a C, then a purine (either A or G) is preferred for X (Figure 2).

Insight into the mode of binding of ET743 to DNA was initially gained through molecular modeling and molecular mechanics techniques using the DNA dodecamer d(CGCT-TGGGAACG)$_2$ as well as different heptamers containing a central GGG, GGC, GGT, TGG, or CGG triplet flanked by two AT base pairs on each side.[6] As a result, both an orientation for bound ET743 in the minor groove and a role for hydrogen bonding in the sequence recognition of DNA by ET743 were suggested. More recently, the covalent complex formed between the closely related ET736 and the oligonucleotide d(CG-TAAGCTTACG)$_2$ was investigated in much greater detail using two-dimensional ^{1}H NMR complemented with 100-ps molecular dynamics (MD) simulations.[4,5] These seminal studies were crucial for understanding the sequence specificity rules described above but they did not reveal any significant disturbances in the conformation of the double helix. Rather surprisingly, however, DNA structural distortions were recently deduced from results of gel electrophoresis experiments that showed ET743

* Corresponding author.
[†] Universidad de Alcalá.
[‡] Pharma Mar S.A.

(1) (a) Wright, A. E.; Forleo, D. A.; Gunawardana, G. P.; Gunasekera, S. P.; Koehn, F. E.; McConnell, O. J. *J. Org. Chem.* **1990**, *55*, 4508−4512. (b) Rinehart, K. L.; Holt, T. G.; Fregeau, N. L.; Stroh, J. G.; Keifer, P. A.; Sun, F.; Li, L. H.; Martin, D. G. *J. Org. Chem.* **1990**, *55*, 4512−4515. (c) Rinehart, K. L. *Med. Res. Rev.* **2000**, *20*, 1−27.

(2) (a) Moore, B. M., II; Seaman, F. C.; Wheelhouse, R. T.; Hurley, L. H. *J. Am. Chem. Soc.* **1998**, *120*, 2490−2491. (b) Corrigenda: Moore, B. M., II; Seaman, F. C.; Wheelhouse, R. T.; Hurley, L. H. *J. Am. Chem. Soc.* **1998**, *120*, 9975.

(3) Pommier, Y.; Kohlhagen, G.; Bailly, C.; Waring, M.; Mazumder, A.; Kohn, K. W. *Biochemistry* **1996**, *35*, 13303−13309.

(4) Moore, B. M. II; Seaman, F. C.; Hurley, L. H. *J. Am. Chem. Soc.* **1997**, *119*, 5475−5476.

(5) Seaman, F. C.; Hurley, L. H. *J. Am. Chem. Soc.* **1998**, *120*, 13028−13041.

(6) Guan, Y.; Sakai, R.; Rinehart, K. L.; Wang, A. H. *J. Biomol. Struct. Dyn.* **1993**, *10*, 793−818.

10.1021/ja000964q CCC: $19.00
Published on Web 07/13/2000

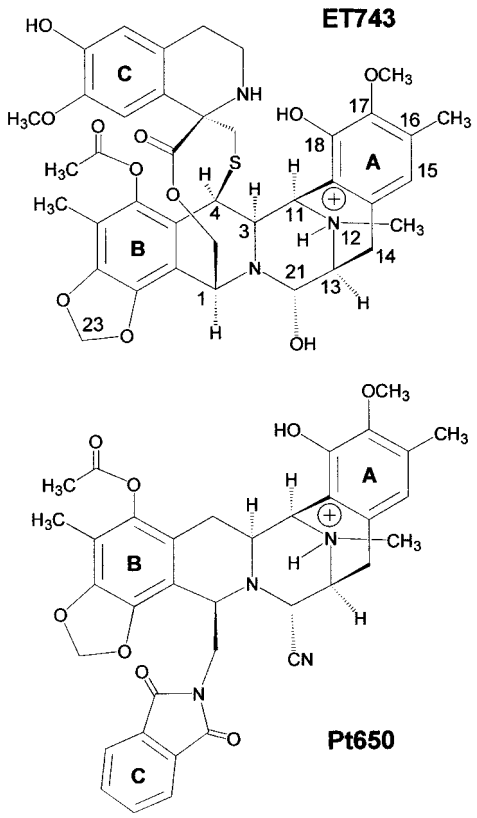

Figure 1. Chemical structures of ecteinascidin ET743 and phthalascidin Pt650. Atoms in ET743 relevant to the discussion have been labeled.

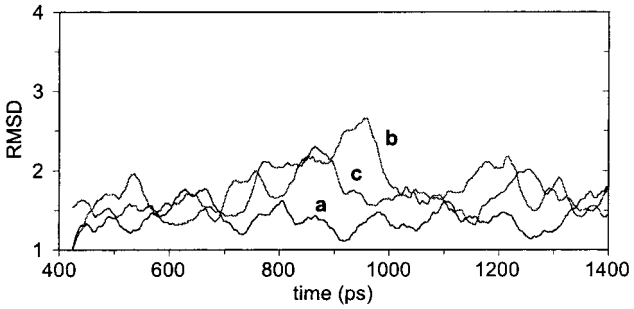

Figure 2. Time evolution (ps) of the root-mean-square deviation (Å) between the simulated structures and the corresponding initial structures (all solute non-H atoms were included in the comparisons) for the (a) AGC-ET743, (b) AGC−Pt650, and (c) CGG-ET743 covalent adducts.

to be the first example of a DNA minor groove alkylator that bends DNA toward the major groove.[7] However, neither the actual site of bending nor the bending mechanism were elucidated in this work.

MD computer simulations constitute a valuable means of developing models and interpreting diverse experimental data on DNA structure in solution,[8] with or without experimentally derived restraints. Recent advances in force-field parameters, simulation methodology, and computer power have made possible the simulation of reliable trajectories in terms of intermolecular forces and motions that give an independent account of experimentally observed behavior, including DNA bending.[9]

In the course of our theoretical studies on the DNA binding selectivity of ET743, we first focused on the non-self-complementary nonamers d(TAA**AGC**TTA)$_2$ and d(TAA**CG-G**TTA)$_2$, hereafter named AGC and CGG, respectively. Each of these oligonucleotides consists of one of the three-base-pair sequences favored by ET743 (shown in bold), as assessed in duplex band shift assays, flanked by an AT-rich triplet on each side. Our interest in modeling these two complexes was that each contains a high-affinity central site representative of the two optimal binding modes for ET743 in the DNA minor groove (Figure 2). Both oligonucleotides in the free state were also simulated as controls. For comparison purposes, the noncovalent complex between ET743 and the low-reactivity sequence d(TAA**CGA**TTA)$_2$ was later included in our studies (referred to as CGA). Despite the fact that it incorporates two successive guanines, albeit on opposite strands, the central triplet CGA has been suggested not to display suitably positioned hydrogen bonding donor/acceptor atoms for optimal stabilization of ET743. Last, the covalent complex between d(TAA**AGC**TTA)$_2$ and phthalascidin (Pt650, Figure 1), a related but totally synthetic molecule, was also studied as this drug has been recently shown to be endowed with the same mode of action and comparable antitumor activity as ET743.[10] The different oligonucleotides are identified in the discussion by the central recognition triplet (shown in bold above).

The molecular level picture provided by our simulations strengthens the belief that ET743 binding to DNA is stabilized in target sequences by specific hydrogen bonds and causes widening of the DNA minor groove, as suggested. In addition, the MD simulations show that, upon covalent binding of ET743 or Pt650 to a central guanine, the twist angle is reduced at this base step and significant positive roll is introduced that results in smooth bending of the DNA oligonucleotide toward the major groove. The degree of bending is consistent with the experimental results and could be relevant for the antitumor action of this class of drugs.

Methods

Force Field and Charges. N12-protonated ET743 and Pt650 (Figure 1) were constructed using the 0.9-Å resolution X-ray structure of the naturally occurring ET743 N12-oxide as a template. Preliminary molecular orbital and continuum electrostatic calculations[11] using MOPAC93-derived[12] ESP charges[13] revealed N12 as the preferred site for protonation (data not shown), in agreement with NMR-based reports for ET743 both in the free state and in a DNA covalent complex.[4,5] Three suitable fragments of each molecule were then used as input for the ab initio quantum mechanical program Gaussian 94.[14] The geometry of each fragment was optimized and RHF 6-31G*\\3-21G* RESP charges[15] were derived together with appropriate bonded and nonbonded

(7) (a) Zewail-Foote, M.; Hurley, L. H. *J. Med. Chem.* **1999**, *42*, 2493−2497. (b) Zewail-Foote, M.; Hurley, L. H. *Anticancer Drug Des.* **1999**, *14*, 1−9.

(8) Beveridge, D. L.; Ravishanker, G. *Curr. Opin. Struct. Biol.* **1994**, *4*, 246−255.

(9) (a) Young, M. A.; Beveridge, D. L. *J. Mol. Biol.* **1998**, *281*, 675−687. (b) Sherer, E. C.; Harris, S. A.; Soliva, R.; Orozco, M.; Laughton, C. A. *J. Am. Chem. Soc.* **1999,** *121*, 5981−5991. (c) Sprous, D.; Young, M. A.; Beveridge, D. L. *J. Mol. Biol.* **1999**, *285*, 1623−1632. (d) Pastor, N.; Pardo, L.; Weinstein, H. *Biophys. J.* **1997**, *73*, 640−652.

(10) Martinez, E. J.; Owa, T.; Schreiber, S. L.; Corey, E. J. *Proc. Natl. Acad. Sci. U.S.A.* **1999**, *96*, 3496−3501.

(11) Nicholls, A.; Honig, B. *J. Comput. Chem.* **1991**, *12*, 435−445.

(12) Stewart, J. J. P. MOPAC 93 1993, Fujitsu Ltd., Tokyo, Japan.

(13) Besler, B. H.; Merz, K. M.; Kollman, P. A. *J. Comput. Chem.* **1990**, *11*, 431−439.

(14) Gaussian 94, Revision E.1, Frisch, M. J.; Trucks, G. W.; Schlegel, H. B.; Gill, P. M. W.; Johnson, B. G.; Robb, M. A.; Cheeseman, J. R.; Keith, T.; Petersson, G. A.; Montgomery, J. A.; Raghavachari, K.; Al-Laham, M. A.; Zakrzewski, V. G.; Ortiz, J. V.; Foresman, J. B.; Cioslowski, J.; Stefanov, B. B.; Nanayakkara, A.; Challacombe, M.; Peng, C. Y.; Ayala, P. Y.; Chen, W.; Wong, M. W.; Andrés, J. L.; Replogle, E. S.; Gomperts, R.; Martin, R. L.; Fox, D. J.; Binkley, J. S.; Defrees, D. J.; Baker, J.; Stewart, J. P.; Head-Gordon, M.; González, C.; Pople, J. A.; Gaussian, Inc.: Pittsburgh, PA, 1995.

Table 1. Comparison of the NOESY Cross-Peak Intensities Reported for the ET736-d(CGTAAGCTTACG)$_2$ Adduct (Ref 5) with the Corresponding Distances (Å) Monitored during the Unrestrained Simulation of the Solvated ET743-AGC Covalent Complex

drug proton	DNA proton	NOESY intensity	mean distance	standard deviation
		Subunit A		
H15	H4′(C7)	1	3.6	0.5
C17OMe	H5″(T21)	3	5.8	0.4
C18OH	H1′(T20)	3	4.7	0.3
	H4′(T20)	1	4.2	0.6
	H4′(T21)	1	4.2	0.5
	H5′(T21)	1	2.9	0.3
	H5″(T21)	1	3.3	0.4
H14B	H4′(C7)	3	3.6	0.3
		Subunit B		
H13	HN2B(G6)	2	3.5	0.1
	H1(G6)	2	4.6	0.1
H21	HN2B(G6)	2	2.8	0.1
	H1(G6)	2	4.3	0.1
	H1′(C7)	3	2.8	0.4
H11	H1′(T20)	3	2.6	0.2
H1	H1′(T20)	3	6.2	0.3
	H1(G6)	2	3.8	0.2
	H1(G18)	3	4.4	0.2
H3	H1(G6)	2	4.7	0.2
H4	HN2B(G6)	3	5.0	0.2

parameters consistent with the AMBER force field,[16] which was updated with new parameters for improved sugar pucker phases and helical repeat.[17] RESP charges were recalculated for the ET743 and Pt650 fragments bonded to guanine and appropriate parameters were assigned to their constituent atoms.

Construction of the Starting Structures. Models of the free oligonucleotides were built using optimized parameters for B-DNA.[18] The noncovalent complex between d(TAAAGCTTA)$_2$ and ET743 was then modeled on the basis of the hydrogen bonding pattern and ^{1}H−^{1}H distance information provided by the NMR experiments on the related ET736-d(CGTAAGCTTACG)$_2$ complex.[5] The strategy consisted of manually placing the drug close to the minor groove in the proposed orientation[5,6] and using MD at 300 K to bring into proximity the atoms shown to give rise to intermolecular NOESY connectivities (Table 1). To this end, weak distance restraints (1 kcal mol^{-1} Å^{-2}) with lower and upper limits of 2−3, 3−4, and 4−5 Å were used during the heating phase (20 ps) for strong, medium, and weak relative intensities of the ^{1}H NOESY cross-peaks, respectively. An upper bound of 5 ± 0.5 Å was also assigned to the distances between atoms involved in intermolecular hydrogen bonds to aid in the positioning of the drug. Distances and angles for the hydrogen bonds involving the DNA bases were reinforced by means of upper-bound harmonic restraining functions with force constants of 10 kcal mol^{-1} Å^{-2} for distances and 30 kcal mol^{-1} rad^{-2} for angles.[19] A harmonic force constant of 5 kcal mol^{-1}Å^{-2} was also applied to the AT terminal bases to constrain them to their initial positions. During the ensuing equilibration and production phase lasting 1000 ps, all the restraints involving ET743 and the central DNA triplet were removed *including* those reinforcing the hydrogen bonds between the base pairs. Nonbonded interactions were calculated for all atom pairs and the solvent environment was simulated by a continuum medium of relative permittivity $\epsilon = 4r_{ij}$. An average structure from the last 250 ps of this simulation was refined by means of steepest-descent energy minimization using a distance-dependent dielectric function, and the resulting complex was considered the initial structure for the MD simulations in water. It is important to highlight the fact that, under the simulation conditions described, removal of the hydrogen bonds between the central base pairs was essential for mutual drug−DNA adaptation and optimal hydrogen-bonding interactions. Otherwise the minor groove did not open up sufficiently to allow deep penetration of subunit B and formation of the hydrogen bond between the methylenedioxy group and the exocyclic amino group of G13.

This noncovalent complex was solvated and subjected to MD as described below, and a representative structure from the simulation in water (after 250 ps of equilibration) was used as a template for modeling an adduct containing a covalent bond between N2 of the central guanine and C21 of ET743. This covalent complex was refined by means of 2000 steps of steepest descent energy minimization keeping all the atoms fixed to their initial positions except those belonging to ET743 and the covalently attached guanine, which were free to move.

The complexes of ET743 with d(TAACGGTTA)$_2$ and d(TAACGATTA)$_2$ were constructed by introducing the appropriate modifications of base composition in the preceding structures followed in each case by energy refinement. Replacement of ET743 with Pt650 in the covalent complex with d(TAAACGTTA)$_2$ was accomplished by suitable modification of the C subunit followed by energy minimization as above.

Molecular Dynamics in Water. Each molecular system was neutralized by addition of the appropriate number of sodium ions,[20] placed along the phosphate bisectors, and immersed in a rectangular box of ∼3000 TIP3P water molecules.[21] Each water box extended 10 Å away from any solute atom, and the cutoff distance for the nonbonded interactions was 9 Å. Periodic boundary conditions were applied and electrostatic interactions were represented using the smooth particle mesh Ewald method[22] with a grid spacing of ∼1 Å. 1.4-ns *unrestrained* MD simulations at 300 K and 1 atm were then run for the free oligos, the noncovalent complexes, and the covalent adducts using the SANDER module in AMBER.[23] SHAKE[24] was applied to all bonds involving hydrogens and an integration step of 2 fs was used throughout. The simulation protocol was essentially as described,[25] involving a series of progressive energy minimizations followed by a 20-ps heating phase and a 70-ps equilibration period before data collection. System coordinates were saved every picosecond for further analysis. Unrestrained MD simulations under similar conditions have been shown to realistically model sequence-dependent structural effects in DNA duplexes[9,26] and to reproduce an NMR-derived nucleic acid structure even when starting from an incorrect structure.[27]

Analysis of the MD Trajectories. Three-dimensional structures and trajectories were visually inspected using the computer graphics program InsightII.[28] Root-mean-square (rms) deviations from the initial structures, interatomic distances, and distribution functions were monitored using CARNAL.[23] The conformational and helical parameters of the DNA nonamers were analyzed by means of program CURVES.[29] The magnitude and directionality of bending was related to the local helicoidal parameters roll and tilt, and quantified in terms of the angle of axis deflection (θ) and its orientation relative to the major groove (ϕ). Display of these quantities for individual base pair steps was

(15) Bayly, C. I.; Cieplak, P.; Cornell, W. D.; Kollman, P. A. *J. Phys. Chem.* **1993**, *97*, 10269−10280.
(16) Cornell, W. D.; Cieplak, P.; Bayly, C. I.; Gould, I. R.; Merz, K. M.; Ferguson, D. M.; Spellmeyer, D. C.; Fox, T.; Caldwell, J. W.; Kollman, P. A. *J. Am. Chem. Soc.* **1995**, *117*, 5179−5197.
(17) Cheatham, T. E.; Cieplak, P.; Kollman, P. A. *J. Biomol. Struct. Dyn.* **1999**, *16*, 845−862.
(18) Arnott, S.; Hukins, D. W. *Biochem. Biophys. Res. Commun.* **1972**, *47*, 1504−1509.
(19) Gallego, J.; Ortiz, A. R.; Gago, F. *J. Med. Chem.* **1993**, *36*, 1548−1561.
(20) Aqvist, J. *J. Phys. Chem.* **1990**, *94*, 8021−8024.
(21) Jorgensen, W. L.; Chandrasekhar, J.; Madura, J. D. *J. Chem. Phys.* **1983**, *79*, 926−935.
(22) Darden, T. A.; York, D.; Pedersen, L. G. *J. Chem. Phys.* **1993**, *98*, 10089−10092.
(23) Pearlman, D. A.; Case, D. A.; Caldwell, J. W.; Ross, W. S.; Cheatham, T. E.; Ferguson, D. M.; Seibel, G. L.; Singh, C.; Weiner, P. K.; Kollman, P. A. AMBER4.1, University of California, San Francisco, 1995.
(24) Ryckaert, J. P.; Ciccoti, G.; Berendsen, H. J. C. *J. Comput. Phys.* **1977**, *23*, 327−341.
(25) (a) Cheatham, T. E.; Kollman, P. A. *J. Am. Chem. Soc.* **1997**, *119*, 4805−4825. (b) Cheatham, T. E.; Srinivasan J.; Case D. A.; Kollman P. A. *J. Biomol. Struct. Dyn.* **1998**, *6*, 265−280.
(26) Cheatham, T. E.; Kollman, P. A. *J. Mol. Biol.* **1996**, *259*, 434−444.
(27) Miller, J. L.; Kollman, P. A. *J. Mol. Biol.* **1997**, *270*, 436−450.
(28) Insight II, version 98.0, 1998. Molecular Simulations Inc.: 9685 Scranton Road, San Diego, CA 92121-2777.
(29) Lavery, R.; Sklenar, H. *J. Biomol. Struct., Dyn.* **1988**, *6*, 63−91.

performed using polar plots ("bending dials")[30] in which θ and ϕ are the radial and angular coordinates, respectively. Points on the northern hemisphere of the dial reflect positive roll and compression of the major groove whereas bending into the minor groove is plotted on the southern hemisphere of the dial. Each ring on our bending dials indicates a 10° deflection of the helical axis, and ϕ runs clockwise from the top.

All calculations were performed on the SGI Power Challenge at Alcalá University Computer Center and locally on SGI O2 workstations. Each MD simulation in water took about 540 h of CPU time.

Results and Discussion

General Considerations. After the equilibration period, the progression of the rms deviations of the coordinates of the solutes with respect to the initial structures (Figure 2) shows that the simulations were long enough to capture the inherent flexibility of the DNA molecules. The absence of drifting to higher rms deviations is suggestive of adequate system equilibration during the sampling time. It is noteworthy that none of the oligonucleotides examined in this work contains any of the typical terminal GC pairs which are usually employed in MD simulations to prevent end-fraying effects.[5,9,25−27] The seven internal base pairs remained well stacked and internally hydrogen bonded in all the duplexes studied despite the absence of any external restraints. End base pairs swinging out into solution were observed most dramatically in the simulations of the free oligonucleotides, which showed first one of the terminal thymines and then the other exchanging their hydrogen bonds to their adenine partners with similar interactions with water. Fraying was most pronounced at the 5′ end of the first strand, as monitored by increases in rise and/or longer inter-base hydrogen bond distances (data not shown). The terminal adenines remained comparatively better stacked over their preceding base pairs, most likely as a result of their larger surface area.

Interestingly, the destabilization of the terminal base pairs in AGC was much less pronounced upon noncovalent binding of ET743 and was almost absent in the ET743-AGC covalent adduct in which all bases conserved their Watson−Crick pairing arrangement for the whole length of the simulation. This behavior was also observed in the ET743-CGG complex. In the Pt650-AGC complex, however, changes in the torsional angles of the sugar−phosphodiester backbone linking T1 and A2 led to partial unstacking of the terminal thymine in this strand after 800 ps. From the limited data it is not possible to generalize to other sequence contexts or longer DNA stretches but the increased terminal base pair stabilization achieved in these oligonucleotides upon binding of ET743 is suggestive of DNA stabilization and merits further study.

The general structure of the complexes (Figure 3) is one in which subunit A of ET743 protrudes perpendicularly off the helix right in front of G5, subunit B stacks over the sugar ring of C14 in a manner reminiscent of that of typical nonintercalative minor groove binders such as Hoechst 33258,[31] and subunit C makes extensive contacts on one side with the sugar−phosphate backbone of the two nucleosides on the 3′ side of G5, whereas the other flat side remains exposed to the solvent.

Prealkylation Binding Complexes. The N12 proton has been proposed to play a role in sequence recognition by ET743 and also to act as an internal catalytic proton that mediates the dehydration of the adjacent carbinolamine moiety to yield the reactive iminium intermediate.[2,4,5] In our simulations of the AGC prealkylation binding complex, the protonated N12 remains hydrogen bonded to the O2 acceptor atom of T15 (Table 2) whereas the carbinol OH acts both as a hydrogen bond donor to O2 of C14 and as a hydrogen bond acceptor from N2 of G5 (Figure 4). The methylendioxy oxygen facing the minor groove is also involved in a hydrogen bond with N2 of G13, and the OH on subunit C is hydrogen bonding alternatively to its neighboring methoxy group and to O1P of the phosphate linking T7 and T8. The OH on subunit A, on the other hand, is not involved in intermolecular hydrogen bonding as its hydrogen points away from the DNA and its closest DNA atom is O3′ of T15, which lies at about 4.0 Å (Table 2).

The consequences of this binding mode are that the interstrand O6(G5)-N4(C14) and N1(G5)-N3(C14) hydrogen bonds are broken and both the opening and the negative propeller twist of the G5-C14 base pair increase (40.5 ± 7.0 and -24.6 ± 9.7, respectively) relative to the free oligonucleotide (1.6 ± 4.6 and -7.4 ± 10.6, respectively) to avoid the steric clash between N1(G5) and N4(C14) (Figure 4). Although this distortion is propagated to the neighboring AT pairs, these bases easily accommodate and the double helical structure is only minimally perturbed except for widening of the minor groove (Table 3) and a net bending toward the major groove. It is remarkable that similarly ruptured hydrogen bonds caused by rotation of the bases have been reported recently in a duplex oligonucleotide with an engineered cross-link in the minor groove between two central guanine bases.[32]

In agreement with the fact that a CGA triplet does not represent a good binding site for ET743,[3] the simulation of the noncovalent complex between ET743 and the CGA duplex did not lead to a suitable geometry for adduct formation. ET743 was initially oriented so as to form hydrogen bonds between the protonated N12 and N3(G15) and between the carbinol OH and N2(G5). During the MD simulation, however, the drug slid one step "upstream" along the minor groove and tried to establish hydrogen bonds between N12 and O2(T16), OH(C21) and N2(G15), and O(methylendioxy) and N2(G5). In this location, ET743 is interacting with the CGT triplet on the opposite strand but is found in an "upside-down" orientation with respect to the AGC complex (Supporting Information). After 900 ps, the C21−N2(G5) distance was ~5.8 Å, as opposed to 3.9 ± 0.2 Å between C21−N2(G5) in the AGC complex (averaged over the last 1000 ps). The longer distance between the two reactive centers, which is critically important to nucleophilic reactivity,[33] largely contributes to making ET743 an unsuitable target for nucleophilic attack by G5 in CGA. The instability of the trajectory, as assessed by the progressive increase in root-mean-square deviation (data not shown), led us to discontinue this simulation after 900 ps. The CGA triplet corresponds to the reverse of the AGC sequence and differs from CGG in only one base pair. However, the absence of an additional 2-amino group in the minor groove on the 3′ side of the central guanine appears to be enough to make CGA a low-affinity site, as suggested.[5] Therefore, the simultaneous occurrence of three hydrogen bonds seems to be critical for stabilization of ET-DNA prealkylation complexes.

Covalent Complex between ET743 and AGC. In the covalent ET743-AGC adduct (Figure 5a), the standard Watson−Crick pairing scheme between G5 and C14 is restored and the

(30) Young M. A.; Ravishanker, G.; Beveridge, D. L.; Berman, H. M. *Biophys. J.* **1995,** *68*, 2454−2468.

(31) Gago, F.; Reynolds, C.; Richards, W. G. *Mol. Pharmacol.* **1989**, *35*, 232−241.

(32) van Aalten, D. M.; Erlanson D. A.; Verdine G. L.; Joshua-Tor, L. *Proc. Natl. Acad. Sci. U.S.A.* **1999**, *96*, 11809−11814.

(33) (a) Menger, F. M. Nucleophilicity and Distance. In *Nucleophilicity*; Harris, J. M., McManus, S. P., Eds.; Adv. Chem. Ser. No. 215; American Chemical Society: Washington; pp 209−218. (b) Ortiz, A. R.; Pisabarro, M. T.; Gago, F. *J. Med. Chem.* **1993,** *36*, 1866−1879.

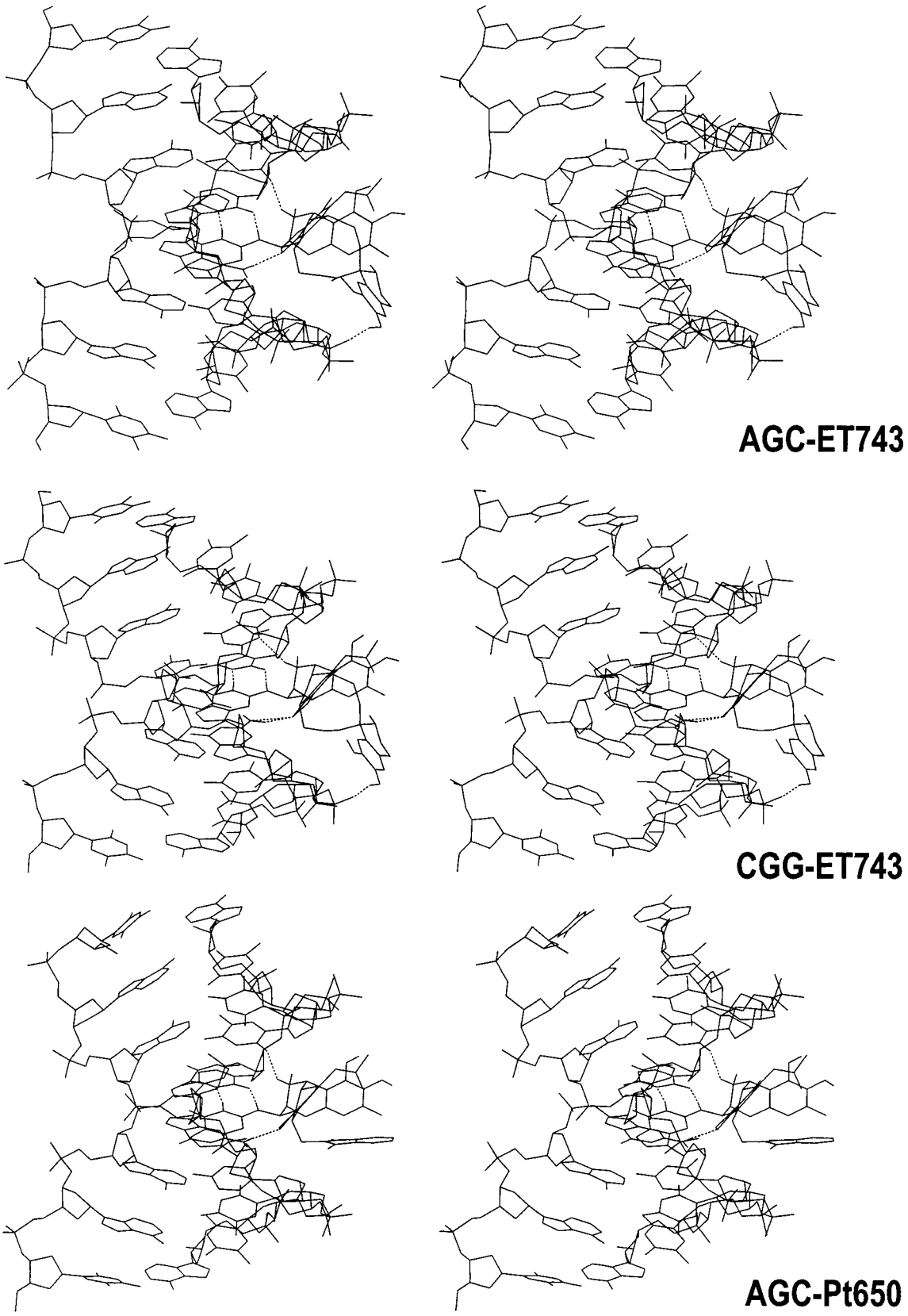

Figure 3. Stereoview of the covalent complexes between (from top to bottom) ET743 and AGC, ET743 and CGG, and Pt650 and AGC. Each complex is a representative refined average structure from the last 500 ps of the MD simulations. Coordinates for the complexes of ET-743 with $d(TAAAGCTTA)_2$ and $d(TAACGGTTA)_2$ have been deposited with the Research Collaboratory for Structural Bioinformatics with PDB identification codes 1EZ5 and 1EZH, respectively, for immediate release.

duplex remains in a stable geometry, as assessed by the monotonically low rms deviation (between 1.0 and 1.5 Å) from the initial structure (Figure 3), in accordance with the NMR observations.[5] The reported intermolecular NOE intensities are entirely consistent with the average inter-proton distances monitored during the MD simulation (Table 1). The H5″(T21)−

Table 2. Intermolecular Hydrogen Bonding Donor−Acceptor Distances (Å) Observed in the AGC Pre-alkylation Complex and the Three Covalent Complexes Studied[a,b]

	ET743-AGC (precov.)		ET743-AGC (cov.)		Pt650-AGC		ET743-CCG	
	mean distance	standard dev	mean distance	standard dev	mean distance	standard dev	mean distance	standard dev
OH−O2(C14)	2.7	0.1						
OH−N2(G5)	2.9	0.2						
N12−O2(T15)	2.8	0.1	2.9	0.1	2.9	0.1		
N12−N3(G15)							3.3	0.2
N2(G13)−OM	3.3	0.4	3.0	0.2	3.0	0.2		
N2(G6)−OM							3.0	0.2
OHC−O1P(T8)	2.8	0.4	2.7	0.2			2.8	0.5
OHA−O3′(T15)	4.6	0.5	3.9	0.4	3.9	0.3		
OHA−O3′(G15)							3.5	0.2

[a] OH is the carbinol hydroxyl oxygen. OM and OHA stand for the methylenedioxy oxygen and the phenolic oxygen from subunit A, respectively. The phenolic oxygen from subunit C (OHC) is also included for comparison (see text for details). [b] Averaged over the last nanosecond of the simulation.

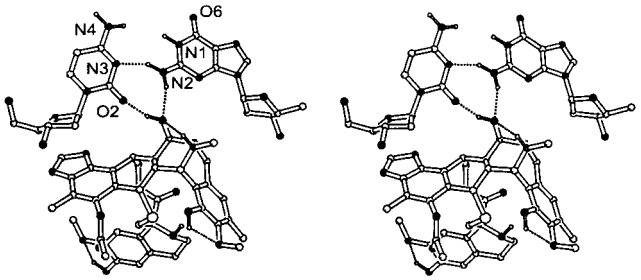

Figure 4. Stereoview showing a detail of the pre-covalent complex between ET743 and d(TAAAGCTTA)$_2$. In place of the three standard hydrogen bonds between G5 and C14, only one involving N2(G5) and N3(C14) remains. Disruption of these hydrogen bonds results in opening of this base pair and an increase in negative propeller twist, which may facilitate subsequent bending. Only hydrogens involved in hydrogen bonds are shown.

Table 3. Width of the Minor Groove (Å) in the Central Part of Each Duplex[a]

	P5−P18	P6−P17	P7−P16	P8−P15	P9−P14
		AGC			
free	6.5 (1.6)	5.9 (1.2)	5.0 (1.1)	4.5 (0.8)	5.2 (0.9)
ET743 (precov.)	4.1 (1.4)	6.6 (0.7)	9.5 (0.4)	8.4 (0.6)	6.8 (1.3)
ET743 (cov.)	5.4 (1.4)	7.9 (0.7)	9.5 (0.4)	8.2 (0.5)	5.9 (1.1)
Pt650	5.3 (1.0)	8.6 (0.9)	9.4 (0.4)	7.3 (0.8)	4.9 (1.2)
		CGG			
free	6.7 (1.6)	6.9 (1.6)	5.8 (1.7)	4.6 (1.5)	5.7 (1.2)
ET743	7.9 (1.4)	7.5 (0.9)	9.4 (0.4)	8.5 (0.7)	6.6 (1.6)

[a] Measured as the shortest inter-phosphate distances across the groove (P−P distance minus 5.8 Å). The P−P distance in canonical B-DNA is 5.9 Å. Mean values obtained from the last 1000 ps of the MD simulations are shown, with standard deviations in parentheses. Measurement of O1′−O1′ distances provides similar relative differences.

C17OMe proton distance is slightly longer than expected for a weak NOESY intensity but this may be due to the fact that during our simulation the methyl of the methoxy group is trapped in an energy minimum on one side of the phenyl ring, as found in the X-ray crystal structure; on the longer time scale of the NMR experiments it is likely that this methoxy group can rotate and populate the alternative conformation, that with the methyl group on the other side of the phenyl ring, bringing it closer to the H5″(T21) proton. As regards the H1 proton of subunit B, we find it closer to H1′(C19) than to H1′(T20) but spin diffusion might possibly account for the weak NOESY intensity assigned to the latter. The hydrogen bonds reported above for N12, the methylendioxy oxygen, and the OH on subunit C are also conserved (Table 2). On the other hand, the OH on subunit A remains in an unsuitable geometry for hydrogen bonding to either O3′ of T15 or O1P of T16, as the separating distance is ∼4.0 Å and the H consistently points toward the ortho methoxy substituent. This phenolic hydroxyl group is known to be essential for the antiproliferative activity of ecteinascicin-like molecules and is presumed to be involved in interactions with DNA binding proteins.[10]

The minor groove in this complex is notably wider than that in the free oligonucleotide (Table 3), in line with earlier qualitative assessments.[5] The ensuing compression of the major groove in the central region and the significant increase in roll mostly localized at the A4/G5 step (Table 4) determine a slightly bent conformation (Figure 3). A decrease in twist angle is also apparent at the A4/G5 step, which is underwound relative to the same step in the free DNA.[34]

Recent ^{23}Na magnetic relaxation dispersion measurements on DNA oligonucleotides have shown that sequence-specific ion binding in the minor groove of AT regions is a rather infrequent and short-lived event.[35] The low occupancies are accounted for by the fact that these bound ions are displaced relatively easily by water molecules: residence times of about 50 ns are calculated for the sodium ions compared to 1 ns for each of the ∼1000 water molecules that bind to the same site before it is occupied again by a cation. To study the behavior of the counterions present in our simulations, we monitored the first and second solvation shells for each sodium ion, as well as the distance between these ions and the most electronegative DNA atoms,[36] that is, the phosphate O1P and O2P oxygens, the N3 and O2 atoms in the minor groove, and the N7 and O6 atoms in the major groove. We found that, after about 400 ps, one sodium ion lost part of its second solvation shell and migrated to the minor groove to remain nearly equidistant from O2(T16), N3(A4), O1′(G5), and O3′(A4) for the rest of the simulation (Figure 6). The relatively long residence time of this counterion in this location (∼1 ns) is indicative of a preferential binding site but this evidence is not enough to suggest that it is playing a role in complex stabilization. The solvation shells of the remaining sodium ions remained more or less constant for the whole length of the simulation, indicating that they belong to the diffuse ion atmosphere that surrounds the drug−DNA complex, and this was also the case for the remaining complexes described below.

Covalent Complex between Pt650 and AGC. Despite the decrease in size, the relative increase in flexibility, and the loss

(34) Gorin, A. A.; Zhurkin, V. B.; Olson, W. K. *J. Mol. Biol.* **1995**, *247*, 34−48.
(35) Denisov, V. P.; Halle, B. *Proc. Natl. Acad. Sci. U S A.* **2000**, *97*, 629−633.
(36) Lavery, R.; Pullman, B. *J. Biomol. Struct., Dyn.* **1985**, *2*, 1021−1032.

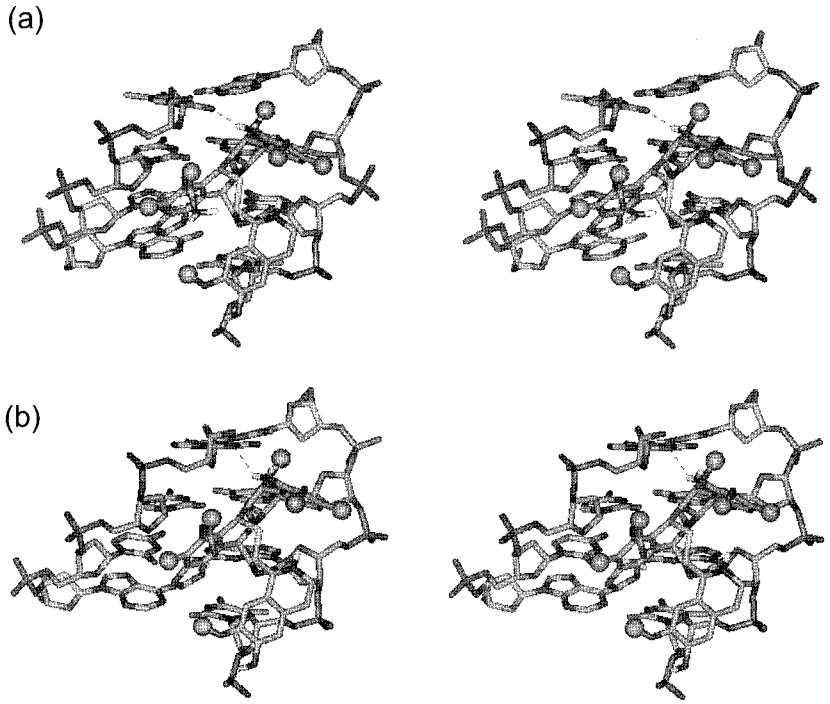

Figure 5. Stereoview of the minor groove in the central region of the (a) AGC-ET743 and (b) CGG-ET743 complexes showing the hydrogen bonds (broken lines) between the drug and the DNA atoms. For clarity, only the DNA segment 4-7:12-15 is shown in each case. Methyl groups are represented as spheres.

Table 4. Comparison of Local Helix Parameters for the Central Four Base Pair Steps Involved in Binding of ET743 and Pt650[a]

	A3:T16/A4:T15			A4:T15/G5:C14			G5:C14/C6:G13			C6:G13/T7:A12		
	twist	roll	slide	twist	roll	slide	twist	roll	slide	twist	roll	slide
						AGC						
X-ray	35.8 (3.1)	0.5 (3.2)	0.0 (0.3)	30.5 (4.9)	2.9 (6.9)	0.5 (0.7)	38.3 (3.8)	−7.0 (6.1)	0.3 (0.4)	30.5 (4.9)	2.9 (6.9)	0.5 (0.7)
free	36.0 (5.0)	0.3 (8.7)	−0.6 (0.5)	32.9 (4.6)	2.3 (7.3)	−1.4 (0.5)	35.8 (4.4)	0.4 (6.7)	−1.5 (0.4)	33.8 (4.6)	2.7 (6.7)	−1.4 (0.5)
ET743	33.2 (4.2)	1.4 (6.4)	−1.2 (0.5)	23.7 (4.7)	16.8 (7.0)	−0.3 (0.4)	36.5 (4.7)	−3.5 (7.6)	−0.5 (0.4)	29.2 (5.2)	3.6 (7.5)	−1.4 (0.4)
Pt650	31.8 (4.5)	2.0 (6.7)	−1.2 (0.6)	22.0 (4.4)	17.9 (7.9)	−0.3 (0.4)	34.4 (4.5)	−1.0 (7.5)	−0.7 (0.4)	31.4 (4.8)	2.8 (7.0)	−1.6 (0.4)
	A3:T16/C4:G15			C4:G15/G5:C14			G5:C14/G6:C13			G6:C13/T7:A12		
	twist	roll	slide	twist	roll	slide	twist	roll	slide	twist	roll	slide
						CGG						
X-ray	30.5 (4.9)	2.9 (6.9)	0.5 (0.7)	31.1 (4.7)	6.6 (3.2)	0.6 (0.3)	33.4 (3.3)	6.5 (2.9)	0.6 (0.0)	30.5 (4.9)	2.9 (6.9)	0.5 (0.7)
free	32.4 (5.2)	−3.8 (10.7)	−0.8 (0.4)	35.7 (5.5)	10.3(8.2)	−0.6 (0.5)	36.0 (5.0)	2.6 (7.6)	−1.3 (0.7)	35.4 (4.1)	−4.1 (6.8)	−1.1 (0.4)
ET743	30.0 (4.8)	2.5 (7.0)	−0.9 (0.4)	34.0 (4.7)	13.6 (9.0)	−0.3 (0.4)	33.4 (5.2)	10.3 (7.3)	−1.1 (0.4)	30.6 (4.2)	0.7 (6.9)	−1.0 (0.4)

[a] Mean values obtained from the last 1000 ps of the MD simulations are shown, with standard deviations in parentheses. Reference values, calculated from 195 dinucleotide steps in 38 crystal structures of free B-DNA (ref 34), are provided for comparison purposes. Angles are given in degrees and the slide in Å.

of the hydrogen bond between the phenolic OH and O1P(T7) in going from subunit C of ET743 to the phthalimide moiety of Pt650, the adduct formed between Pt650 and AGC presents very similar structural characteristics (Figure 3) and helical parameters to those described above for the ET743-AGC complex (Table 4). Most noteworthy is the almost perfect overlap of one of the phthalimide oxygens of Pt650 and the carbonyl oxygen of the ester group linking subunits B and C in ET743 when both complexes are superimposed (Figure 7). The rms deviation for all DNA atoms in the central triplet of the ET743-AGC and Pt650-AGC complexes (computed for a representative average structure of each complex) is only 0.3 Å. This structural similarity underscores the importance of the common A and B subunits in DNA recognition and binding, and suggests that ET-743 and Pt650 may be causing roughly the same degree of distortion in their DNA target sites. The conformational stability of the phthalimide moiety may seem remarkable in view of the flexible nature of the methylene linker joining it to the B subunit, but it must be realized that rotation of the ring is hindered by the rest of the molecule and the DNA sugar−phosphate backbone on which it sits (Figure 3).

Covalent Complex between ET743 and CGG. The evolution of the rms deviation along the trajectory showed that the CGG-ET743 complex is also stable, in agreement with the fact that CGG represents an alternative optimal binding site for ET743.[3] The intermolecular hydrogen bonding scheme found in CGG-ET743 (Table 2) coincides with that originally proposed[5] and differs substantially from that reported above for AGC-ET743. This is a consequence of the different location of hydrogen bond donor and acceptor groups in the minor groove of both sequences on each side of G5. Thus, the protonated N12 is engaged in a hydrogen bond with the N3 acceptor atom of G15, the methylendioxy oxygen facing the minor groove is involved in a hydrogen bond with N2 of G6, and the OH on subunit C is hydrogen bonding to the O1P of the phosphate linking T7 and T8 (Table 2).

Despite the similar overall characteristics of AGC-ET743 and CGG-ET743 complexes (Figure 5), there exist significant

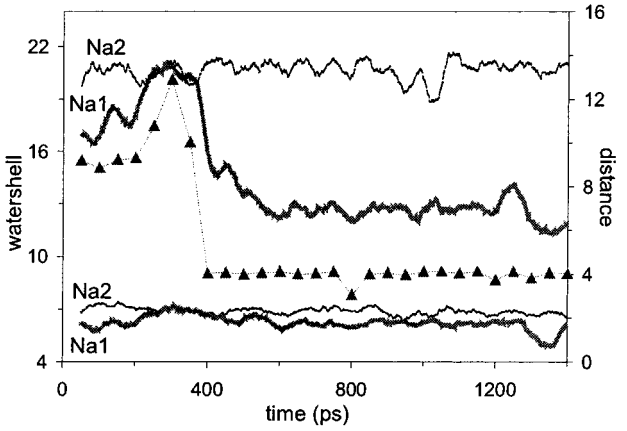

Figure 6. Partial desolvation of a sodium ion (Na1) during the MD simulation of the AGC-ET743 complex. Another sodium ion (Na2) is used as representative of the rest. Left vertical axis: Number of waters in the first and second solvation shells of the sodium ions. Right vertical axis: Shortest distance (▲, Å) between Na1 and either O2(T16) or N3(A4) DNA atoms.

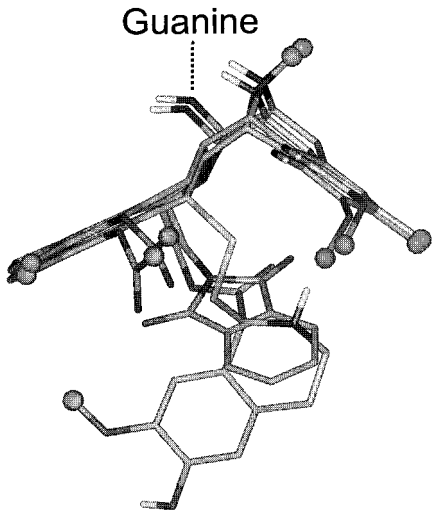

Figure 7. Stick representation of ET743 and Pt650 superimposed in their respective complexes with AGC (methyl groups are represented as spheres). Note the overlap of one of the phthalimide oxygens of Pt650 and the carbonyl oxygen of the ester group linking subunits B and C in ET743.

differences in several local DNA helical parameters (Table 4). Most noteworthy are that no further underwinding is apparent at the C4/G5 step (a naturally underwound step), and that the increase in roll is spread over two consecutive steps (C4/G5 and G5/G6) rather than being localized only on the 5′ side of the alkylated guanine.

Sugar Puckering and Backbone Conformation in the Covalent Complexes. Monitoring of the pseudorotation phase angles (*P*) for the sugar rings revealed only a few significant changes in puckering in going from free to complexed DNA. All of the values were within the $144 \leq P \leq 180°$ range typical of B-DNA conformations (C2′-*endo* family) except for C14 which was found alternating between a C3′-*endo* and a O1′-*endo* conformation in the three covalent complexes.

More changes were observed in the glycosyl torsional angle, χ, of the covalently modified deoxyguanosine in the AGC complexes (Figure 8). This angle ($\sim -120°$ for purine and pyrimidine nucleotides in B-DNA) reflects the orientation of the O1′ atom of the sugar relative to the base, and is changed due to the presence of the bulky drug covalently bonded to G5

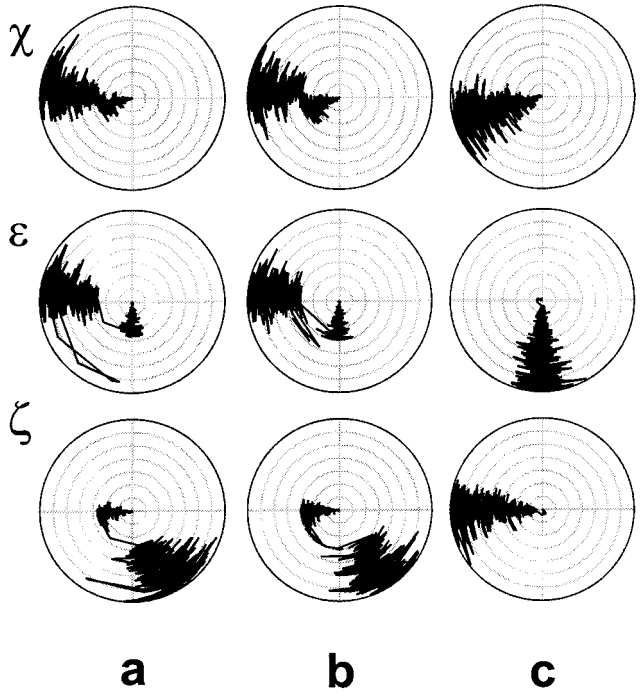

Figure 8. Polar plots for three relevant torsion angles involving G5 in the covalently modified complexes: (a) AGC-ET743, (b) AGC-Pt650, and (c) CGG-ET743. Each ring represents 100 ps in the MD simulation starting from the origin, and each quarter is a 90° interval for the angle values, which run clockwise from 0° at the top of the dial.

in the minor groove. The fact that it does not change in the CGG complex (Figure 8c) reflects the different DNA environment of the methyl group attached to N12 of the drug in the two sequences: it is positioned very close (~4 Å) to the purine C2 atom of A4 in the AGC complexes with ET743 and Pt650 but is farther apart (~6 Å) from the equivalent pyrimidine C2 atom of C4 in the CGG-ET743 complex (Figure 5). In this latter case, the methyl group is close (~3.7 Å) to the exocyclic amino group of G15 in the second strand but it appears that accommodation in this location can be achieved with no additional local distortion.

These changes in the torsion angle values of the G5 glycosyl bond are coupled to changes in the backbone torsional angles ϵ (C4′−C3′−O3′−P) and ζ (C3′−O3′−P−O5′), which normally exhibit the largest structural variability in DNA and are in turn correlated to each other.[37] In the AGC-ET743 and AGC−Pt650 complexes, after about 600 ps, the change in χ from 240° to 280° is accompanied by a crankshaft motion of the backbone affecting ϵ and ζ that corresponds to a transition from the standard B_I conformation to B_{II} (Figure 8). In the CGG-ET743 complex, on the other hand, the backbone at G5 remains essentially unchanged in the same conformation as in free DNA (B_I) but at C4 we find frequent B_I-B_{II} transitions that are somewhat stabilized in favor of B_I upon binding of ET743 (data not shown). Interestingly, these alternative conformations have been detected in the 1.1 Å resolution X-ray structure of a 2:1 complex of daunomycin with the oligonucleotide $d(CGCGCG)_2$ in which each drug molecule appears covalently linked to the N2 of a central guanine.[38]

DNA Bending in the Covalent Complexes. In the study of static X-ray crystal structures, DNA bending can be easily

(37) Bertrand, H.; Ha-Duong, T.; Fermandjian, S.; Hartmann, B. *Nucleic Acids Res.* **1998**, *26*, 1261−1267.

(38) Schuerman, G. S.; Van Meervelt, L.; Backbone, *J. Am. Chem. Soc.* **2000**, *122*, 232−240.

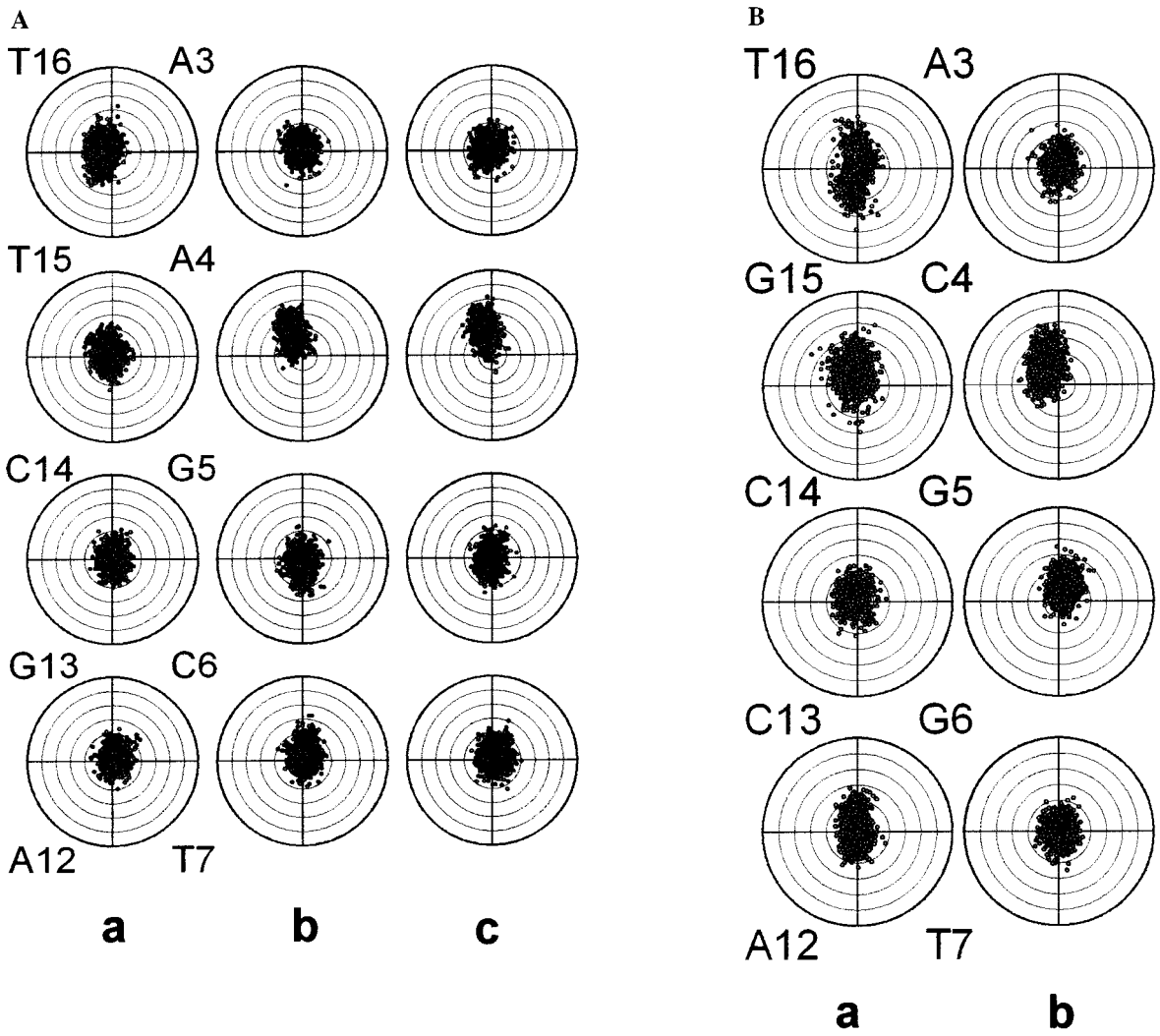

Figure 9. Polar plots ("bending dials") for the four consecutive steps involved in drug binding at the center of each DNA molecule: **A**, (a) AGC, (b) AGC-ET743, and (c) AGC-Pt650; **B**, (a) CGG and (b) CGG-ET743. Individual points are for structures separated by 1 ps throughout the course of the trajectory, and viewed together they constitute a probability density. Bending compressing the major groove is plotted on the northern hemisphere of the dial.

quantified in terms of the angle formed between the helical axis vectors for the first and last base-pairs of the sequence and/or as the percentage shortening of the helix end-to-end distances. During a MD simulation, however, transient fluctuations of the overall helical axis at multiple points during the trajectory make these measurements subject to considerable background noise.[9] This dynamic component, indicative of conformational substates,[39] is aggravated in the case of short DNA sequences, especially when fraying affects some of the sequences to be compared. For these reasons we have found it more rigorous and useful to focus on the central part of the oligonucleotides where each drug binds.

A convenient pictorial representation of each of the four central DNA steps is provided in the form of bending dials,[30] which are polar plots that display both the magnitude and the direction of the helical bend (Figure 9). Bending compressing the major groove, which arises from the positive roll reported in Table 4, is clearly apparent at the A4/G5 step in the AGC-ET743 and AGC-Pt650 complexes and is of comparable magnitude in both (Figure 9, a and b). This bending direction on the 5′ side of the covalently modified guanine does not change over time whereas the direction of bending for the same step in the free DNA used as control is much more variable with no discernible preference so as to cancel out when averaged over time. The tendencies of the G5/C6 and C6/T7 steps in these two complexes, on the other hand, are not very different from those of the equivalent steps in the free DNA, and do not imply significant additional bending. As regards CGG, the C4/G5 step is consistently bent toward the major groove in both the free CGG nonamer and the CGG-ET743 complex whereas the G5/G6 step bends in this same direction only as a consequence of drug binding.

In relation to these findings, it is illustrative to compare our results with those obtained from a survey of X-ray crystal structures.[30] The G/C step was shown to bend almost exclusively into the minor groove in the case of dodecamers but this tendency was not evident in the case of decamers, which is in consonance with the present results for the AGC nonamer. The C/G step, in turn, which is highly represented in X-ray experimental structures, was identified as the only pyrimidine/purine step that demonstrates a significant bias toward bending into the major groove, which is also in agreement with the values reported here. All homopurine steps in X-ray crystal structures, except G/A, demonstrate a preference for bending in the direction of the major groove. Additionally, they display negative tilt values indicative of bending into the sugar−

(39) McConnell, K. J.; Nirmala, R.; Young, M. A.; Ravishanker, G.; Beveridge, D. L. *J. Am. Chem. Soc.* **1994**, *116*, 4461−4462.

phosphate backbone of their complementary Watson−Crick pyrimidine−pyrimidine steps. In our simulated free oligonucleotides, the A3/A4 and A4/G5 steps in AGC, and the G5/G6 step in CGG, all show this direction of compression (apparent as dots on the left hemisphere of the dial). Upon binding of ET743 or Pt650, this tendency is clearly increased in A4/G5 but is slightly reduced in A3/A4 and reversed in G5/G6. These differences arise from the particular geometries enforced by the distinct hydrogen bonding patterns detected in the complexes (Figure 5). The additional tilt component compressing the complementary strand is also apparent at the C4/G5 step in the AGC complexes. In all cases, therefore, a clear bend toward the major groove can be noted that is even more pronounced in the case of the CGG-ET743 complex due to its apparently greater intrinsic bending propensity. A quantitative measure of bending can be obtained by computing with CURVES the angles between the base normal vectors from one side of the binding site (A3:T16) to the other (T7:A12) during the last nanosecond of the MD trajectories: $14.5 \pm 5.5°$, $18.6 \pm 6.1°$, and $24.3 \pm 5.0°$ for the AGC-ET743, AGC-Pt650, and CGG-ET743 complexes, respectively. The value for AGC-ET743 compares well with the $17 \pm 3°$ experimentally calculated for this sequence.[7] As for the origin of the bend, it has been shown that it is possible to bend the DNA progressively toward the major groove by gradually changing the torsion angle values of the glycosyl bond.[9d] We observe such changes in χ localized at G5 but only in the AGC complexes. Since the CGG complex is seen to bend even to a greater extent without significant changes in this parameter, this explanation appears unlikely in this case. Another possible contribution may come from the replacement of the high dielectric solvent with the low dielectric environment of the drug, which could bring about an increased repulsion between the phosphates across the minor groove.[40] Although this possibility is attractive and merits further study, the increase in minor groove width and the bend toward the major groove can be easily accounted for by strictly mechanical reasons: a wedge effect due to occupancy of the minor groove and increases in roll at one (AGC) or two (CGG) steps.

The simulations of the covalent complexes reported here involve a relatively short piece of DNA and a nanosecond time scale. Longer MD trajectories simulating longer DNA oligonucleotides of precise sequence in the absence of bound ligands have demonstrated curvature reversals.[9] In our case, however, bending is mostly due to the presence of a covalently bonded drug in the minor groove and is likely to be permanent, which could be important for modulating the functions of the DNA molecule.

Biological Implications. The exact mechanism by which ecteinascidins and related compounds exert their rather unique cytotoxic action[10] has not been completely elucidated yet. DNA bending and minor groove widening, as shown here to occur in the covalent complexes of ET743 and Pt650 with two different DNA sequences, could be important for either enhancing or impairing recognition by transcription factors or some other DNA binding proteins. By inducing bends in DNA, the drug could be serving a surrogate protein function[7] by bringing specified fragments not contiguous in primary sequence closer together, and this may result in enhanced recruitment of specific and nonspecific binding proteins. In this regard, the phenyl ring of subunit A and the hydroxyl group attached to it, both of which have been shown to be important for activity,[10] could provide suitable anchoring points for hydrophobic and polar interactions with one or several protein residues on the minor groove side. Alternatively, some other proteins might bind on the major groove side taking advantage of the existing bend.[7] Another binding signature that could be recognized by specific proteins is provided by the reported geometrical changes in the sugar−phosphate backbone, which give rise to an electrostatic potential pattern different from that of canonical B-DNA (data not shown).

Unusually wide minor grooves and localized bends brought about by chemical modification are found, among others, in disulfide cross-linked DNA[32,41] and in cis-platinated DNA.[42] These enforced bends can be recognized, for example, by architecture-specific proteins possessing high mobility group (HMG) domains. In this case, recognition is mainly achieved through partial side-chain intercalation into the minor groove, in common with different DNA binding proteins involved in transcriptional regulation.[43] We presume that this type of protein−DNA interaction would be precluded in the present case due to occupancy of the minor groove by the drug, but we note a structural parallel in the manner these proteins and ET743 induce DNA distortions.

ET743 and related compounds could also act by preventing protein binding. This may occur if the protein needs to bend DNA in a direction incompatible with the drug-induced bend or if the cognate sequence for the protein is occluded by the drug. In this regard, the CCAAT box, found in the forward or reverse orientation (i.e. ATTGG), is one of the most common elements in eukaryotic promoters.[44] Among the various transcription factors that interact with this sequence, only the evolutionary conserved activator NF-Y (CBF, HAP2/3/4/5) absolutely requires all five nucleotides.[44] Interestingly, binding of trimeric NF-Y to this sequence has been shown to be inhibited by ET743.[45] Indeed, the TGG triplet is a good binding site for ET-743,[3] and we note that additional binding sites (including AGC triplets) are present on both sides of the CCAAT box in different promoters. For example, the human MDR1 gene contains the sequence CCC**AGC**CAATC**AGC**CT.[44] This raises the possibility of multiple binding sites for ET743 in a relatively short DNA stretch and increased bending if these binding sites are properly phased. Other possibilities cannot be ruled out at present either as there are indications that inhibition of NF-Y binding to DNA by ET-743 may not require previous interaction of the drug with the DNA.[45]

Conclusions

MD simulations have shed further light on the structural modifications brought about in two short DNA molecules upon binding of ET743 or Pt650 and subsequent adduct formation. Each target sequence studied represents a fraction of a DNA helical repeat and is shown to deviate from a straight helix when studied in a dynamic context with different intrinsic bendabilities being apparent for AGC and CGG. The covalently bound antitumor drugs studied impose restrictions in some of the bending motions of free DNA and favor others in such a way

(40) (a) Travers, A. A. *Nat. Struct. Biol*. **1995**, *2*, 615−618. (b) Elcock, A. H.; Potter, M. J.; McCammon, J. A. In *Computer Simulation of Biomolecular Systems*; Van Gunsteren, W. F.; Weiner, P. K.; Wilkison, A. J., Eds.; Kluwer/ESCOM: Dordrecht, 1997; Vol. 3, pp 244−261.

(41) Wolfe, S. A.; Ferentz, A. E.; Grantcharova, V.; Churchill, M. E.; Verdine, G. L. *Chem. Biol.* **1995**, *2*, 213−221.

(42) Ohndorf, U. M.; Rould, M. A.; He, Q.; Pabo, C. O.; Lippard, S. J. *Nature* **1999**, *399*, 708−712.

(43) Werner, M. H.; Gronenborn, A. M.; Clore, G. M. *Science* **1996**, *271*, 778−784.

(44) (a) Mantovani, R. *Nucleic Acids Res.* **1998**, *26*, 1135−1143. (b) Mantovani, R. *Gene* **1999**, *239*, 15−27.

(45) Bonfanti, M.; La Valle, E.; Fernandez-Sousa Faro, J. M.; Faircloth, G.; Caretti, G.; Mantovani, R.; D'Incalci M. *Anticancer Drug Des.* **1999**, *14*, 179−186.

that the net result is a distinct bending toward the major groove. The conformational changes involved are shown to be subtly different in the noncovalent and covalent complexes of ET743 with AGC and relatively similar among the three covalent adducts studied. CGG appears to accommodate the drug with less distortion due to the intrinsic bendability and decreased twist angle of the C/G step and the slightly wider minor groove. This "pre-organization" could facilitate specific recognition by ET743. We would anticipate a similar behavior for the sequence TGG (=CCA), which is part of the CCAAT box in different promoters.

The sequence CGA, which contains a single mismatch relative to CGG, has also been shown to be a poor binding site for ET743. This highlights the importance of hydrogen bonding in the tight fitting of subunits A and B into the minor groove. The bulk of these subunits opens up the minor groove while concomitantly compressing the major groove. Despite the local fluctuations in helical parameters reported in Table 4 for the central base steps and the widened minor groove (Table 3), most of the deformation induced by the drug is absorbed by conformational changes in the sugar−phosphate backbone and base pair parameters of the neighboring residues. This may account for the reported lack of significant distortions in the original ^{1}H NMR work.[5]

It is likely that simulations with longer sequences extended to substantially longer times will highlight other aspects of the interaction of ecteinascidins and related molecules with DNA. In any case, the simulations reported here are useful in that they have allowed us to gain insight into the local bending elements that produce the macroscopic curvature detected in the electrophoretic gel migration and cyclization kinetics experiments.[7]

Acknowledgment. This paper is dedicated to Professor W. G. Richards (Oxford, UK) on the occasion of his 60th birthday. We thank the University of Alcalá Computing Centre for a generous allowance of computer time on a SGI Power Challenge server and the anonymous reviewers for useful comments.

Supporting Information Available: A figure showing a comparative view of the pre-covalent complexes between ET743 and the AGC and CGA oligonucleotides (PDF). This material is available free of charge via the Internet at http://pubs.acs.org.

JA000964Q